CONF-970568--10

ELASTIC MODULUS CALCULATIONS FROM LOAD/DISPLACEMENT CURVES USING SPHERICAL AND POINTED INDENTERS

L. Riester, M. K. Ferber, and K. Breder
High Temperature Materials Laboratory
Oak Ridge National Laboratory,
Oak Ridge, TN. 37831-6069
R. J. Bridge
University of Connecticut
Storrs, Conn. 06269-3222

ABSTRACT

Hard materials with known mechanical properties were probed with spherical and Berkovich indenters using a Nanoindenter(TM). A simple analysis of the loading portion of the indentation experiment was found to give reasonable estimates of the elastic modulus for a variety of brittle materials.

INTRODUCTION

When indentation methods are used to measure the elastic properties of a hard material, there is wide disagreement as to whether it is preferable to use pointed, spherical, or flat bottomed indenters.[1-4] The advantages to using pointed diamond indenters are that their shapes conform more readily to the natural facets of diamond, and they can be calibrated to account for small imperfections in manufacturing.[1] On the other hand, pointed indenters may be less suited for measuring the elastic properties of multilayered coatings and thin films. The advantage of a spherical indenter over the sharp tips is that plasticity is delayed to greater indentation depths which makes it well suited to measure elastic properties. The disadvantages of using a spherical diamond indenter are that it is extremely difficult to manufacture a diamond indenter that conforms to a perfect spherical shape. This makes calibration to offset imperfections very controversial. Swain et al. have used spherical indenters successfully and have managed to calculate aberrations due to imperfections in the shape.[3,4] Based on these theoretical premises and experimental methods, this study attempts to measure the elastic modulus of a variety of materials with known mechanical properties using two spherical and one Berkovich indenter.

BACKGROUND

The simplest indentation experiment which can be performed is that using a spherical indenter. The indentation can remain completely elastic up to a relatively high indentation load, at which point cracking or plastic deformation may occur. The theory of two elastic bodies in contact was originally described by Hertz[5], hence, Hertzian indentation. The elastic stress field beneath the indenter is symmetrical and well described, and a full solution for the three dimensional stress field has been reported.[6,7] The most common use of the Hertzian indentation has probably been the Brinell hardness test, in which the

DISCLAIMER

plastic deformation after spherical indentation provides a measure of the material hardness. This test has long traditions, primarily as an empirical test, but has been set on solid theoretical foundations by Hill et al.[2] The Hertzian test has also been used to determine the fracture toughness,[8-11] again utilizing the well defined symmetrical stress field and the development of ring and cone cracks. Recently, Swain et al.[4] have combined the new depth-sensing hardness testing equipment (mechanical microprobe) with spherical indenters, and implemented elastic/plastic indentation mechanics to determine mechanical properties of thin films. However, very little work utilizing the elastic part of the Hertzian indentation cycle seems to be available in the literature. This is a somewhat puzzling fact since it is a very straightforward experiment with solid theoretical base as described above. Yoffe[12] explored the use of Hertzian indentation for large deformations, i.e., the very practical situation of indenting a highly elastic (rubber) solid with spheres, and corrections to the Hertzian solutions for large deformations were given. Zeng et al.[13] used Hertzian indentation to determine the elastic modulus of several brittle materials by utilizing the well known relationship between the contact area and the elastic constants for the materials. This approach required a measurement of the contact area, and a method for doing this was devised. With the use of the depth sensing indentation devices, another option for measuring the elastic modulus becomes available, utilizing the relationship that exists between elastic indentation depth and elastic constants. This is the approach taken in this paper.

Hertzian theory readily provides the following relationships between the contact radius and elastic constants:

$$a = \left(\frac{3PR}{4} \frac{1}{E^*} \right)^{\frac{1}{3}} \tag{1}$$

where a is the elastic contact radius, P the indentation load, R the radius of the indenter and E* the "composite Modulus" given by:

$$\frac{1}{E^*} = \frac{1-\nu_1^2}{E_1} + \frac{1-\nu_2^2}{E_2} \tag{2}$$

Here ν and E are Poisson's ratio and Young's modulus, respectively, and the subscripts 1 and 2 refer to the indenter and test material, respectively. The maximum elastic deformation δ is likewise given as:

$$\delta = \left(\frac{3P}{4R^{\frac{1}{2}}} \frac{1}{E^*} \right)^{\frac{2}{3}} \tag{3}$$

and in the case of small elastic deformation the relationship between the contact area and contact depth is a function of the indentation sphere radius only:

$$a = (R\delta)^{\frac{1}{2}} \quad (4)$$

Hence, using a depth sensing indentation system with a spherical indenter of known mechanical properties, the elastic modulus of the test material can be obtained assuming the Poisson's ratio is known. For highly elastic materials indented with a stiff indenter, Yoffe[12] found reasonable agreements assuming infinite stiffness of the indenter.

EXPERIMENTAL

Indentations were made with a Nanoindenter I (Nano Instruments) on chips of glass, silicon and sapphire and on metallographically polished specimens (0.5 μm) of fused silica, polycrystalline aluminum oxide, silicon nitride, sintered α-silicon carbide and titanium alloy (for microscopy only). Two spherical diamond indenters (20 μm and 2 μm radius) were purchased from Synton/Imetra. The Berkovich indenter was supplied by Nano Instruments. Single cycle indents were made using load control with loads of 24, 48, 72 and 100 mN; a record of load, displacement and time from each indent was stored. The loading segment from each load vs. displacement curve was extracted. Ten indents from each material which corresponded to the lowest load were averaged. The portion of the loading curve which was linear on a plot of load vs. $\delta^{3/2}$ (5mN or less) was considered for the calculations of the modulus since only that portion could be assumed to constitute the region of elastic contact.

Scanning electron microscopy (Hitachi S-800) and a Scanning Force Microprobe (Topometrix) techniques were used to examine impressions produced by the various indenters in a soft titanium alloy. To avoid errors introduced by the SFM, indents of varying sizes were sampled and scanned in several directions. Both forward and reverse scans were examined. Measurements of the depth and width of the indentations were made using the Topometrix software to determine the radius of the spherical indenters and for direct comparison to the load/displacement curve which provided data on the actual plasticity/elastic recovery of the indentation process.

RESULTS AND DISCUSSION

Nanoindentation

By looking for inflection points on a plot of load vs. δ^2 in the loading curve of the load-displacement cycle, it was relatively easy to determine the regions where the indentations were completely elastic or where some plastic deformation had started to occur. A plot of load vs. $\delta^{3/2}$, on the other hand, was linear even for loads in the plastic region of the indentations, unexpectedly so for the Berkovich indenter (see Fig. 1). This allowed for a more direct comparison to be made between the three indenters. Since a plot of load vs. $\delta^{3/2}$ was linear, the Berkovich indenter was assumed to be spherical in the region of elastic contact even though sphericity was not actually observed in the microscopic images (Figs. 2 and 3). From the fits of indentation vs. elastic deformation, the elastic modulus was determined using Eq. 3.

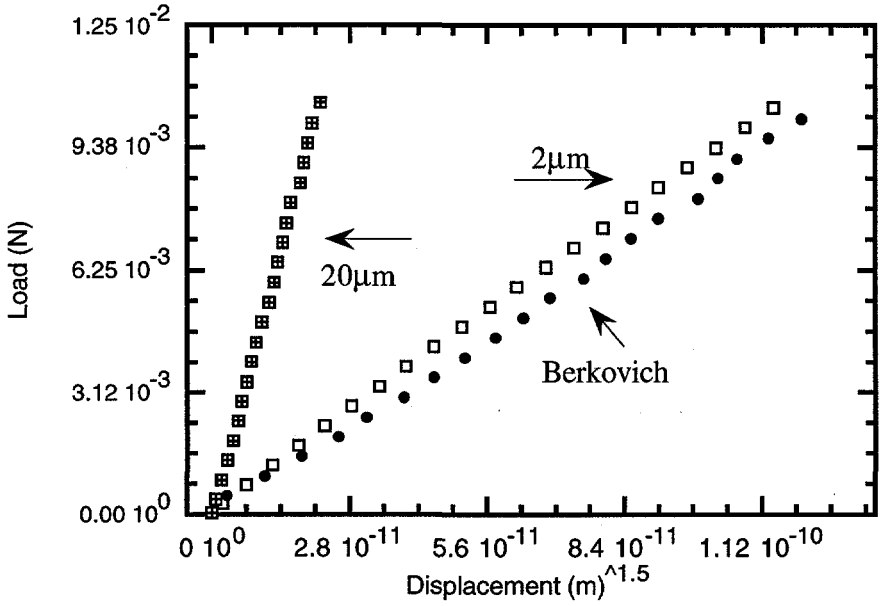

Fig. 1. Load vs. elastic deflection for the three indenters.

As a first assumption, a Poisson's ratio of 0.17 was assumed for all materials since there was some uncertainty about the values to be used for some of the materials. Table I lists the calculated values. The Elastic Modulus and Poisson's ratio for the indenter (diamond) were set to 1140 GPa and 0.07 respectively. The radii of the indenters were as specified by the manufacturer.

From the results in Table I it is apparent that the results are only partially reasonable, and that the 2 µm indenter underestimates the moduli while the 20 µm indenter overestimates the moduli. It is further apparent that the assumption of an infinitely stiff indenter (Yoffe) is relatively good for the low modulus materials (fused silica and glass).

Following Swain[4], the possible reasons for the differences in the moduli were explored, and the most reasonable assumption was that the actual radii of the indenters were not those quoted by the manufacturer. To investigate this possibility, the radius of the indenter was treated as a variable in the calculations of standard materials with the result that elastic moduli were forced to conform to literature values. Table II illustrates the effect on modulus measurements if the shape of all indenters is assumed to be spherical and if the radius is varied to obtain standard values. Results from the pointed Berkovich indenter are included for comparison.

Table I. Elastic moduli calculated using the nominal values of the indenter radii.

Material	E-Modulus* 20 μm Indenter [GPa]	E-Modulus+ 20 μm Indenter [GPa]	E-Modulus* 2 μm Indenter [GPa]	E-Modulus+ 2 μm Indenter [GPa]	E-Modulus# Berkovich Indenter [GPa]
Silicon Nitride	397.9	293.10			348.00
Sapphire	497	343.60	285.10	227.00	486.90
Alumina	501.1	345.60	260.90	211.40	490.90
Glass	91.7	84.70	42.00	40.50	81.20
Fused Silica	86	79.80	50.20	48.00	71.40
Silicon	193.2	164.60	106.00	96.80	180.20
Sintered SiC	422.5	306.30	284.80	226.80	488.80

* Hertz Theory
+ According to Yoffe,[12] assuming infinitely stiff indenter.
# According to Oliver and Pharr method.[1]

Table II. Elastic Moduli calculated using the best fit values of the indenter radii.

Material	E-Modulus* 27μm Rad. Indenter (GPa)	E-Modulus* 1μm Rad. Indenter (GPa)	E-Modulus* 0.5μm Rad. Berkovich (GPa)	E-Modulus# Berkovich from unload. (GPa)
Silicon Nitride	326.21		273.71	348.00
Sapphire	402.71	451.03	379.33	486.90
Alumina	405.84	408.69	367.27	490.90
Glass	77.99	60.38	80.02	81.20
Fused Silica	73.19	72.28	83.84	71.40
Silicon	162.32	156.12	144.27	180.20
Sintered SiC	345.35	450.50	422.52	488.80

*Hertz Theory
According to Oliver and Pharr method[1]

Microscopy

Microscopy was undertaken to obtain measurement which conformed reasonably well to the actual dimensions of the radii of the indenters. A soft titanium alloy was selected for this purpose because it has only minimal elastic recovery when indented which makes it easy to study residual impressions. Electron Microscopic images of impressions of the three different indenters into

a titanium alloy are shown in Fig. 2. It was clearly seen that the 2 μm spherical indenter did not conform to a shape which qualifies as spherical even at low loads. Rather it seemed that the spherical tip was ground from a four-sided pyramid. A side view of the indentation site also showed material pile-up. The 20 μm spherical and the Berkovich indenters appeared to have the expected shapes.

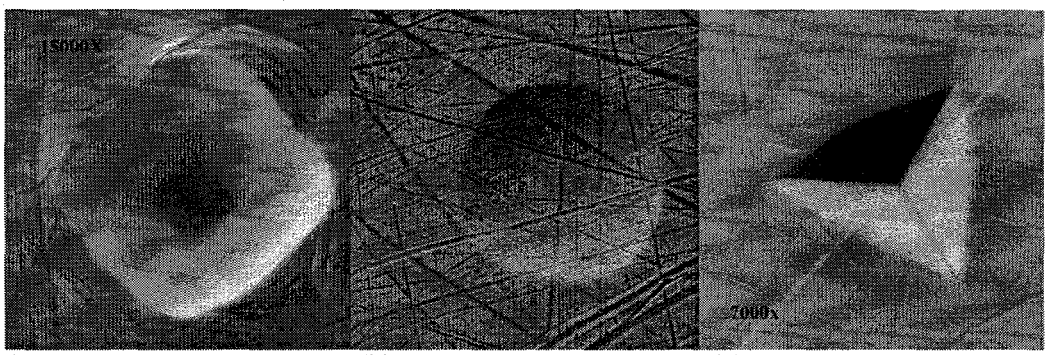

(a) (b) (c)

Fig. 2. SEM images of indents from a 2 μm(a), a 20μm(b), and a Berkovich(c) indenter in titanium alloy.

Further inspection of the indentation sites with the Scanning Force Microprobe revealed that only the Berkovich indenter conformed to the expected shape, see Fig. 3. The 2 μm radius spherical indenter was very irregular. The four sides of the pyramidal shape could be traced to within about 300 nm of the end of the tip. The 20 μm spherical indenter was actually tri-lobal as judged by the material piled up which could easily be determined with the amplification in the z-direction of the SFM. Furthermore, at the very tip there seemed to be a very small residue of a three-sided pyramid or facet. In addition, the indenter tip showed many other irregularities.

By measuring software generated cross sections of the SFM images from the impressions in the titanium alloy, estimations of the actual radii of the two spherical indentations were made. This was a time consuming and difficult task, especially for the smaller indenter for which the impressions were definitely not spherical. Measurements of several indentations were made, and the radius of the nominally 20 μm indenter was found to be 41 μm and the radius of the nominally 2 μm indenter was found to be 2.7 μm. Using these values in the equations for calculating the elastic moduli resulted in the values shown in Table III. To keep it simple, elastic recovery, which was proportional to the area of surface contact, was disregarded in this study. The elastic recovery portion of the indentation contributed to the reported larger diameter measurements in Table III.

Table III. E modulus calculated using the measured sphere radii.

Material	E-Modulus* 41 μm Indenter [GPa]	E-Modulus+ 41 μm Indenter [GPa]	E-Modulus* 2.7μm Indenter [GPa]	E-Modulus+ 2.7μm Indenter [GPa]
Silicon Nitride	250.9	204.7		
Sapphire	305.9	240	236.9	195.4
Alumina	308.2	241.4	217.5	181.9
Glass	62.5	59.1	36	34.9
Fused Silica	58.7	55.7	42.9	41.3
Silicon	128.2	115	90.1	83.3
Sintered SiC	264.8	213.9	236.7	195.2

*Hertz Theory
+ According to Yoffe,[12] assuming infinitely stiff indenter.

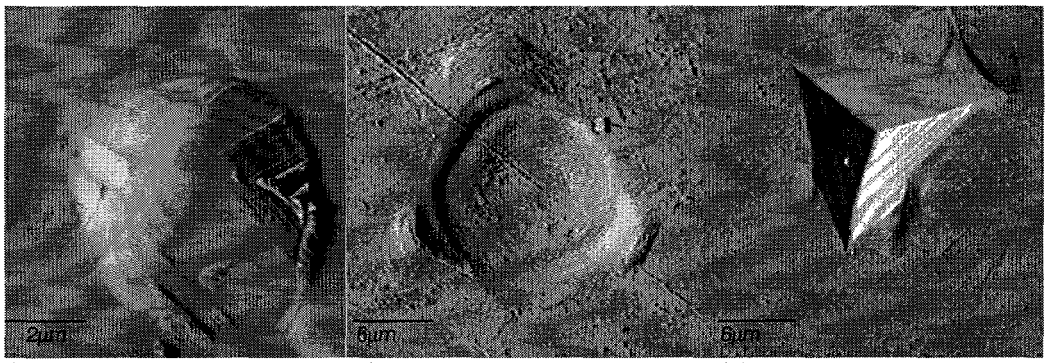

(a) (b) (c)
Fig. 3. SFM images of indents from a 2μm(a), a 20μm(b) and a Berkovich(c) indenter in titanium alloy.

SUMMARY

It is entirely possible to measure the elastic modulus of any material using a spherical or just about any shape indenter in the Nanoindenter. The experimental procedures need some refinement; for example, more data points at very low loads will help avoid errors in calculating the slope of the loading curve. There also was a transition observed in the load/displacement curves on the soft titanium alloy when the indenter "switched" shapes during penetration. Because of the irregular shape even at the very tip, it is difficult to assess how much surface area of the indenter is actually in contact with the substrate in the elastic region of the indentation process. Despite these difficulties, if indenters are carefully characterized, and if constants are calculated based on standard materials, blunt or spherical indenters are useful tools in obtaining elastic moduli of extremely thin films where large surface area contact is needed rather than penetration.

ACKNOWLEDGEMENT

Research sponsored by the U. S. Department of Energy, Assistant Secretary for Energy Efficiency and Renewable Energy, Office of Transportation Technologies, as part of the High Temperature Materials Laboratory User Program, under contract DE-AC05-84OR21400 with Lockheed Martin Energy Research Corp.

REFERENCES

[1]W. C. Oliver and G. M. Pharr, "An improved technique for determining hardness and elastic modulus using load and displacement sensing indentation experiments," J. Mater. Res. **7** [6] 1564-1583, 1992.

[2]R. Hill, B. Storåkers and A. B. Zdunek, "A theoretical study of the Brinell hardness test," Proc. Roy. Soc. A **423** 301-330, 1989.

[3]J. S. Field and M. V. Swain, "A simple predictive model for spherical indentation," J. Mater. Res. **8** [2] 297-306, 1993.

[4]M. V. Swain and J. Mencik, "Mechanical property characterization of thin films using spherical tipped indenters," Thin Solid Films **253**, 204-211, 1994.

[5]H. Hertz, "Hertz's Miscellaneous Papers," Chapters 5 and 6. Macmillan, London 1896.

[6]M. T. Huber, "Zur Theorie der Berührung fester elastischer Körper," Ann. Physik **14** 153-163, 1904.

[7]A. Kelly and N. H. Macmillan, **Strong Solids**, 3rd edition, Clarendon Press, Oxford, 1986.

[8]B. R. Lawn, J. Appl. Phys, **39** 4828, 1968.

[9]R. Warren, "Measurements of the fracture properties of brittle solids by Hertzian indentation," Acta Metall. **26** 1759-69, 1978.

[10]K. Zeng, K. Breder, and D. J. Rowcliffe, The Hertzian stress field and formation of cone cracks - I. Theoretical approach," Acta Metall. Mater. **40** [10] 2595-2600, 1992.

[11]K. Zeng, K. Breder, and D. J. Rowcliffe, The Hertzian stress field and formation of cone cracks - II. Determination of fracture toughness," Acta Metall. Mater. **40** [10] 2601-2605, 1992.

[12]E. H. Yoffe, "Modified Hertz theory for spherical indentation," Phil. Mag. A, **50** [6] 813-828, 1984.

[13]K. Zeng, K. Breder, D. J. Rowcliffe, and C. Herrström, "Elastic modulus determined by Hertzian indentation," J. Mater. Sci. **27** 3789-3792, 1992.